Load shifting versus manual frequency reserve: Which one is more appealing to flexible loads?

Peter A.V. Gade*[1,2], Trygve Skjøtskift[2], Henrik W. Bindner[1], and Jalal Kazempour[1]

[1] *Department of Wind and Energy Systems, Technical University of Denmark, Kgs. Lyngby, Denmark*
[2] *IBM Client Innovation Center, Copenhagen, Denmark*

December 13, 2022

Contents

*Corresponding author. Tel.: +45 24263865.
Email addresses: pega@dtu.dk (P.A.V. Gade), Trygve.Skjotskift@ibm.com (T. Skjøtskift), hwbi@dtu.dk (H.W. Bindner), jalal@dtu.dk (J. Kazempour).

Nomenclature

IS In-sample.

Abbreviations

OOS Out-of-sample.

Abstract

Change something here in Overleaf and push to repo.

1 Introduction

2 Literature review

Test that I can refer to OOS and IS.

3 Monetizing flexibility

3.1 mFRR

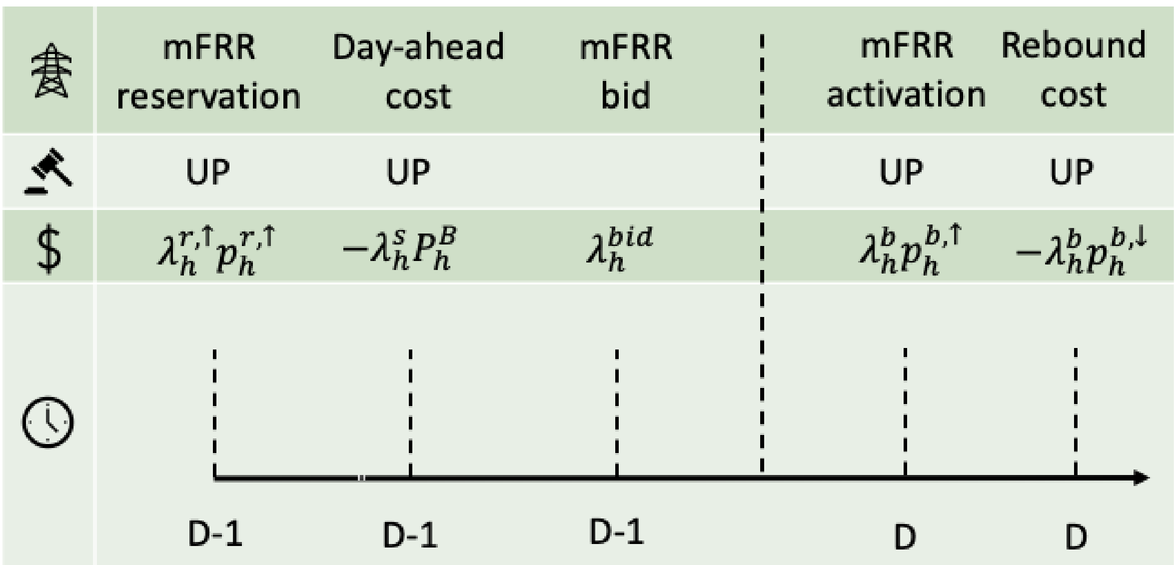

Figure 1: Timeline of cost components in (??).

3.2 Load shifting

4 Grey-box modelling

Most - if not all - of this goes to appendix

4.1 Prediction error method vs simulation errors

5 Thermostatically controlled loads

TCLs are characterized by being controlled such that the temperature is kept at a specified setpoint. Examples includes heat pumps, freezers, air condition units, ovens, etc. They are widely believed to constitute an important part of demand-side flexibility due to the inherent thermal inertia of such temperature-driven systems.

In this paper, we focus on freezers, which are a common type of TCL. Specifically, we focus on a single freezer display in a Danish supermarket. Freezers are characterized by a large thermal inertia due to the frozen food, which makes them suitable for flexibility. On the other hand, the there is a risk of food degradation when utilizing flexibility. Therefore, it is important to model the temperature dynamics in the freezer for a realistic estimation of its flexibility.

The rest of the section is organized as follows. First, we visualize the most important measurements from a real supermarket freezer. Second, we introduce a second-order model that characterizes the supermarket freezer. Third, we validate the second-order model and show how it can be used to simulate a demand response from a freezer.

5.1 Visualization of freezer measurements

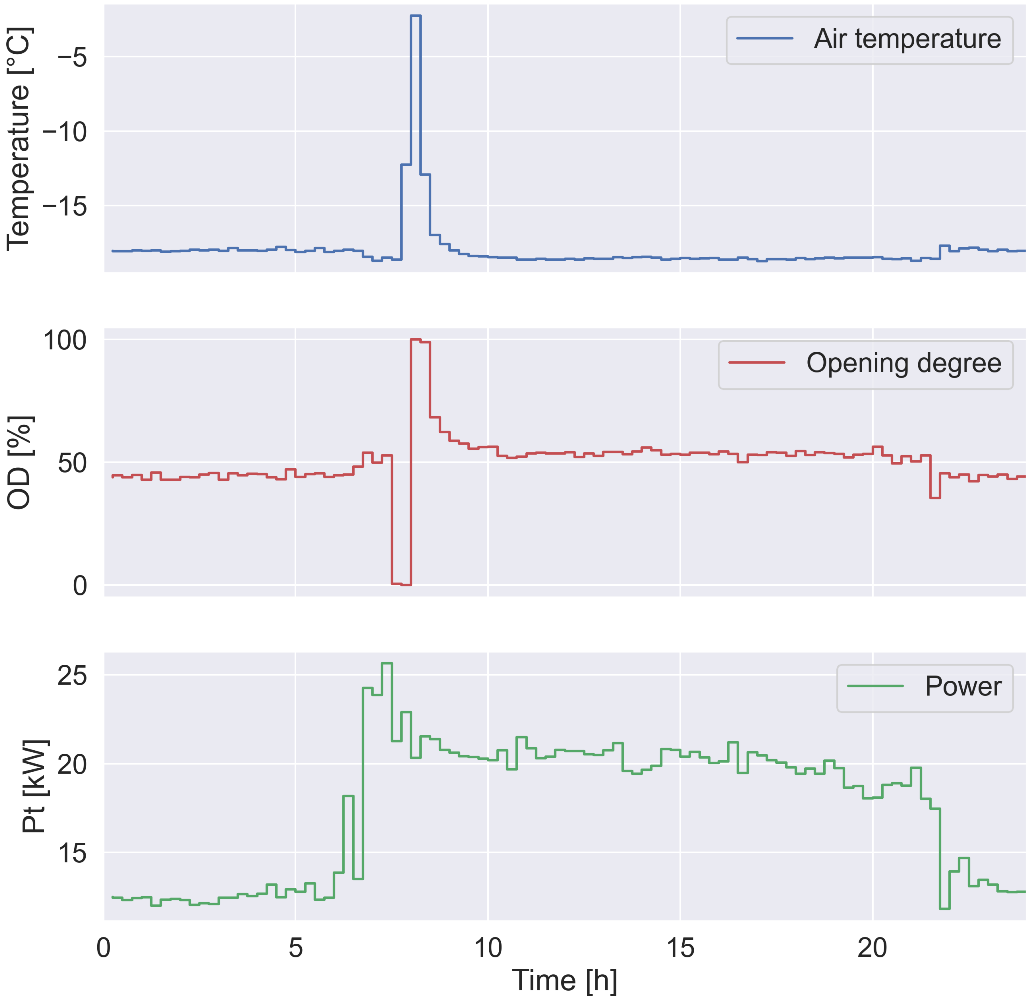

Figure 2: **Top**: yearly average temperature of a single freezer in a supermarket. **Middle**: opening degree of the freezer expansion valve. **Bottom**: power of the compressors feeding all the freezers (scaled to only include all freezers in the supermarket).

5.2 Thermal modelling of freezer

In Appendix A, it is described how a simple TCL model can be made. We extend it to a second-order model that accounts for the thermal mass of the food, which essentially provides the flexibility in freezers:

$$\frac{dT^f(t)}{dt} = \frac{1}{C^f}\left(\frac{1}{R^{cf}}(T^c(t) - T^f(t))\right) \tag{1a}$$

$$\frac{dT^c(t)}{dt} = \frac{1}{C^c}\Big(\frac{1}{R^{cf}}(T^f(t) - T^c(t)) + \frac{1}{R^{ci}(t)}(T^i(t) - T^c(t)) - \eta \cdot OD(t)P(t)\Big) + \epsilon \mathbb{1}^{df} \tag{1b}$$

In state-space form, it is:

$$T^f_{t+1} = T^f_t + dt \cdot \frac{1}{C^f}\left(\frac{1}{R^{cf}}(T^c_t - T^f_t)\right) \tag{2a}$$

$$T^c_{t+1} = T^c_t + dt \cdot \frac{1}{C^c}\Big(\frac{1}{R^{cf}}(T^f_t - T^c_t) + \frac{1}{R^{ci}_t}(T^i_t - T^c_t) - \eta \cdot OD_t P_t\Big) + \epsilon \mathbb{1}^{df} \tag{2b}$$

Here, T^c is the air temperature in the freezer, and T^f is the food temperature which is a latent, unobserved state. It is essentially a low-pass filter of the air temperature in the freezer with time constant $\tau = C^f R^{cf}$. C^f and C^c are the thermal capacitance of the food and air in the freezer, respectively. R^{cf} and R^{ci} are the thermal resistance between food and air, and air and indoor temperature, respectively. Furthermore, ϵ represents the temperature change when defrosting and $\mathbb{1}^{df}$ is an indicator for when defrosting happens. R^{ci} is time-varying to capture the differences between opening- and closing hours. The opening degree, OD_t, and power P_t, are exogenous inputs.

5.3 Validation and simulation

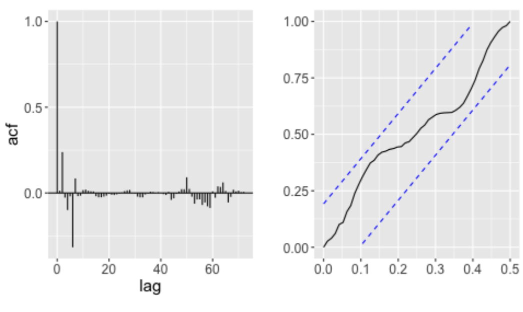

(a) Validation of the state-space model in (2). Left: auto-correlation function of the model residuals. Right: cumulated periodogram of the residuals.

Parameter	Value	Unit
C^f	5.50	kWh/°C
C^c	0.13	kWh/°C
R^{cf}	4.91	°C/kW
$R^{ci,day}$	25.6	°C/kW
$R^{ci,night}$	46.5	°C/kW
η	2.38	
ϵ	6.477	°C/h

(b) Parameter estimates of eq. (2).

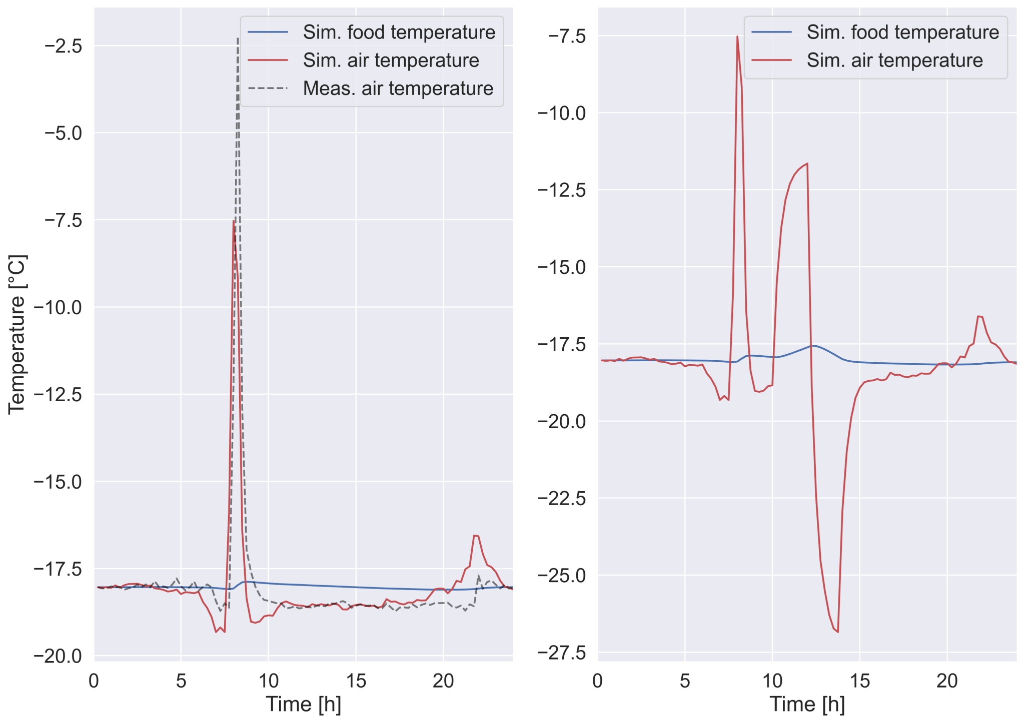

Figure 4: **Left**: Simulation of (2) using the parameters in Table 3b **Right**: Simulation where power is turned off for two hours with a subsequent rebound at the nominal power until the food temperature is back to its normal value.

6 Optimization model

6.1 Objective function

6.2 Scenario generation

6.3 Decomposition

Write about ADMM to solve the optimization problem.

7 Results

7.1 ADMM

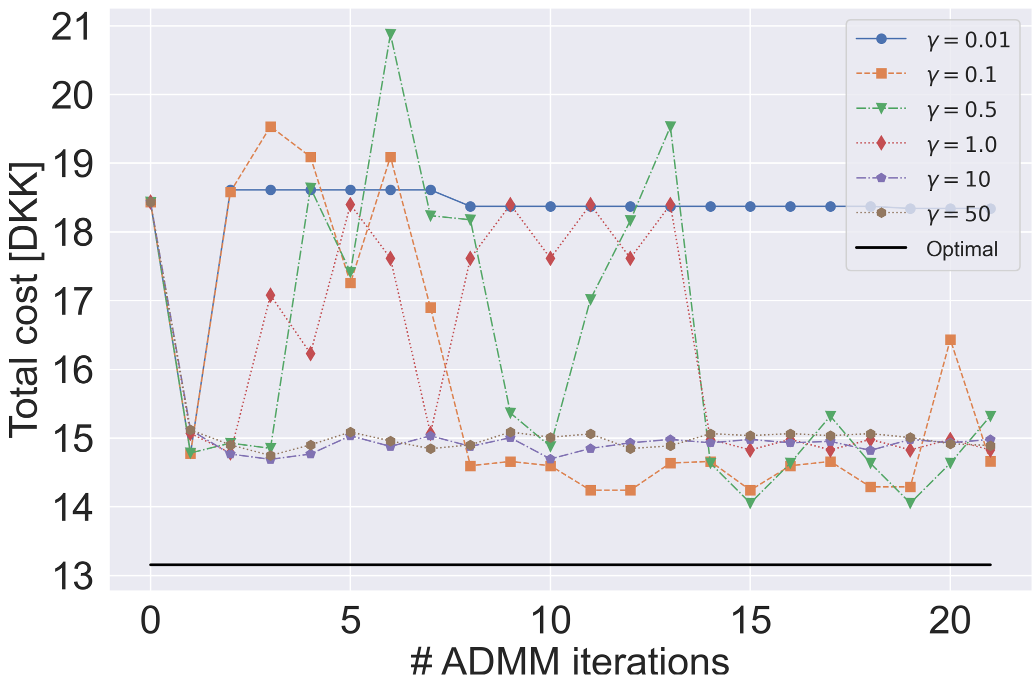

Figure 5: ADMM solution versus the optimal solution for five scenarios.

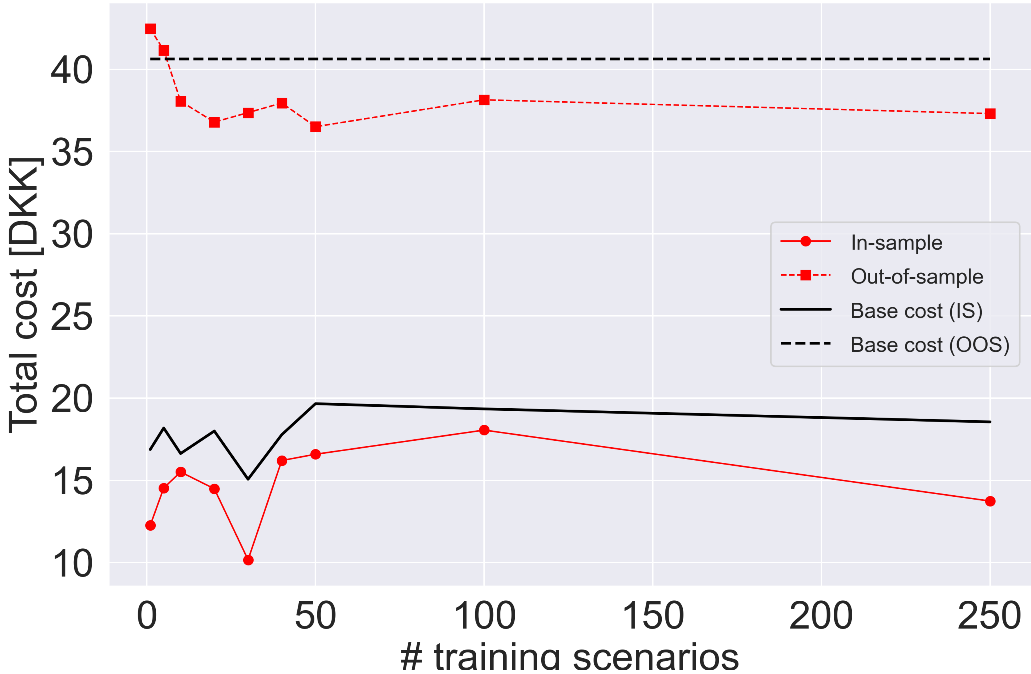

Figure 6: Effect of number of in-sample scenarios on out-of-sample performance for ADMM. Both are compared to the baseline costs of the freezer.

7.2 Lookback

TODO: create plot of effect of lookback parameter.

7.3 Load shifting vs mFRR

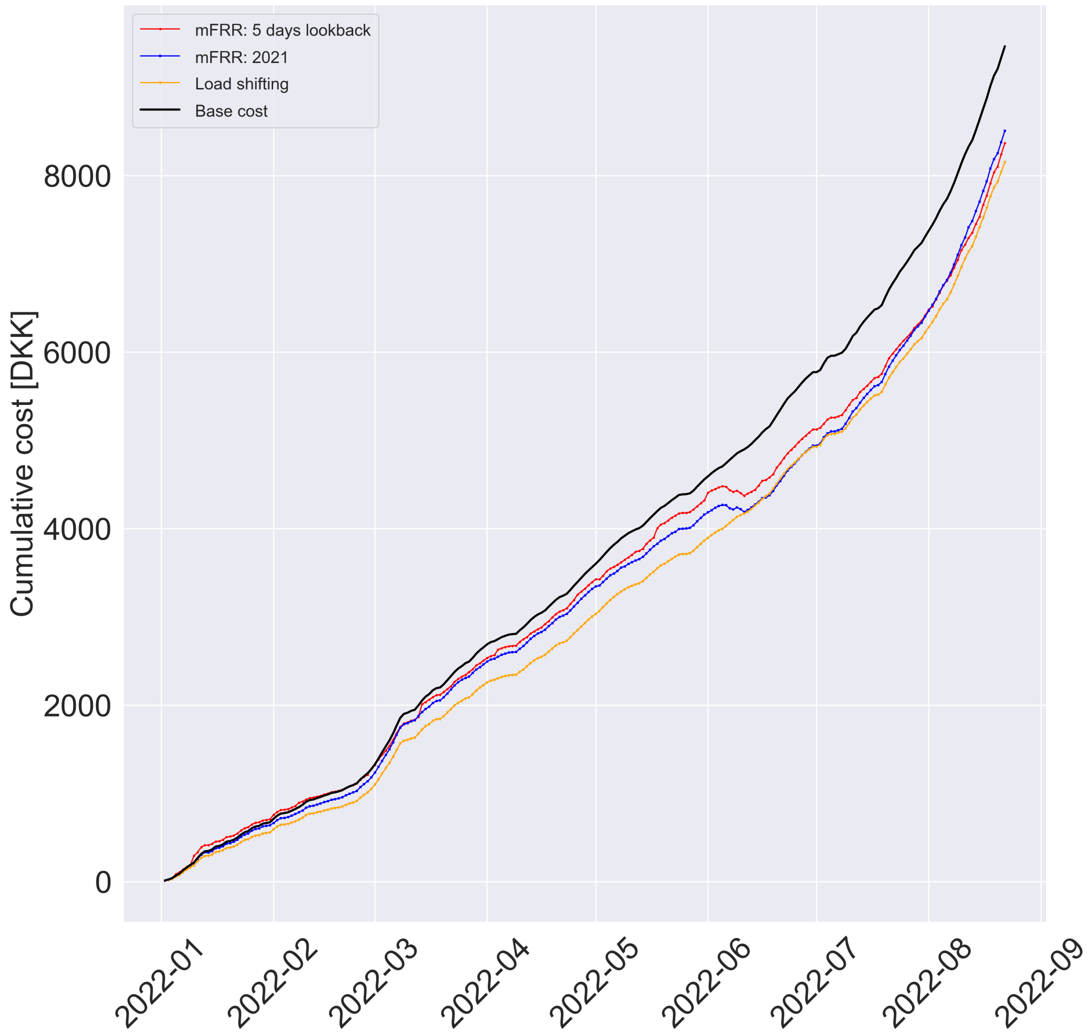

Figure 7: Out-of-sample cumulative costs for load shifting and mFRR using ADMM with 50 scenarios and a lookback of 5 scenarios.

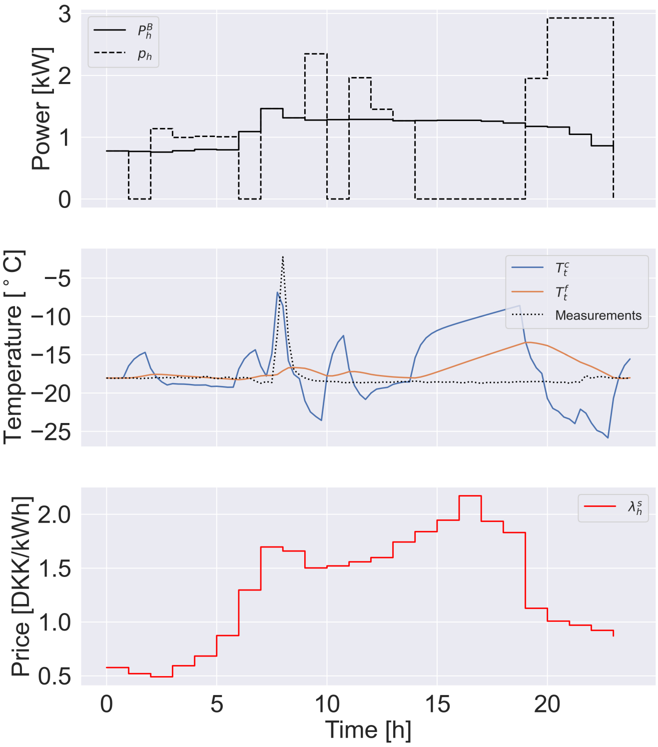

(a) **Top**: Power profile when load shifting and baseline power of freezer. **Middle**: Air and food temperature dynamics. **Bottom**: Spot price in scenario.

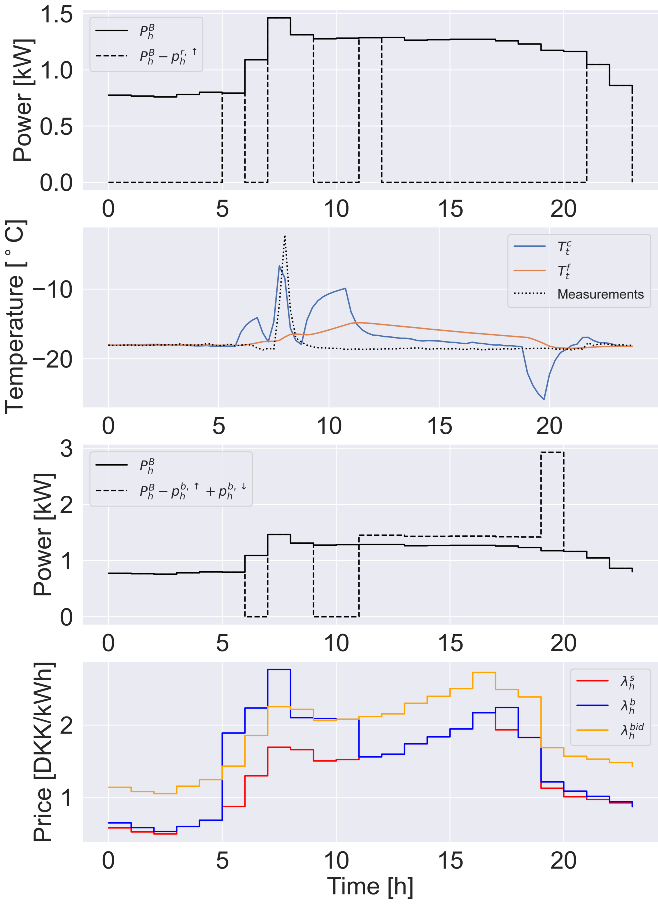

(b) **Top**: Reservation capacities and baseline power of freezer. **Upper middle**: Air and food temperature dynamics. **Lower Middle**: mFRR activations in this scenarios, i.e., when $\lambda_h^{bid} \leqslant \lambda_h^b$ and $\lambda_h^b > \lambda_h^s$ and $p_h^{r,\uparrow} > 0$. **Bottom**: Spot price, balancing price, and bid in scenario.

Figure 8: Comparison between load shifting and mFRR in one scenario in-sample. **Left**: Load shifting. **Right**: mFRR.

Table 1: Out-of-sample costs of freezer in [DKK/day] for mFRR with five days lookback, load shifting, and mFRR trained with 50 in-sample scenarios using ADMM.

Name	mFRR w. lookback	Load shifting	mFRR w. 2021
Base cost today	40.628	40.628	40.628
Total cost	35.918	34.994	36.514
Expected energy cost	40.628	34.994	40.628
Rebound cost	0.858	92.869	0.911
Reserve payment	3.216	0.0	3.381
Act payment	8.092	0.0	2.161
Penalty cost	5.741	0.0	0.516
Scenarios	-5	1	50
Admm	False	False	True
% savings	11.6	13.9	10.1

8 Discussion

9 Conclusion

Test that I can refer to OOS and IS.

Appendices

A Appendix

Hao et al. [1] describes how a TCL can be modelled as a virtual battery using a first-order thermal-electric ODE:

$$\frac{dT(t)}{dt} = \frac{1}{C}\left(\frac{1}{R}(T^a(t) - T(t)) + \eta P(t)\right) \tag{3}$$

Here, $T(t)$ is the temperature, C is the thermal capacitance (kWh/°C), R is the thermal resistance (°C/kW), η is the coefficient of performance (COP), i.e., the cooling/heating effect, $P(t)$ is the power to the TCL, and $T^a(t)$ is the ambient temperature outside the TCL (typically around 20 °C in an indoor environment).

Note, (3) can readily be formulated in a deterministic, state-space model as in (**??**). The following difference equation yields the Euler approximation of (3) which can be used in an optimization model (with the same time step dt):

$$T_{t+1} = T_t + dt \cdot \left(\frac{1}{C}\left(\frac{1}{R}(T_t^a - T_t) + \eta P_t\right)\right) \tag{4}$$

Eq. (3) and (4) constitutes the most simple model of a TCL one can imagine, but, nevertheless, has a quite powerful interpretation: the rate of change of temperature is determined by the heat flux to the surrounding environment and the heat flux from the power source to the TCL. It thus captures the most fundamental temperature dynamics of a TCL.

The steady-state power in (3) is given by:

$$P^{ss}(t) = \frac{T^a(t) - T(t)}{\eta R} \tag{5}$$

The steady-state power is thus the power required to keep the temperature of the TCL constant with respect to the outside temperature, $T^a(t)$, given the efficiency of the system and the thermal resistance. A better energy efficiency can be achieved by either 1) increasing the mechanical efficiency of the cooling/heating system or 2) increasing the thermal resistance to the outside temperature by, e.g., insulating a freezer.

The drawback of the first-order model in (3) is that it is only parameterized by three parameters, and it excludes disturbances. Hence, it might not be an accurate model of a real system. The model can easily be extended to include more complicated dynamics such as heat exchange with a barrier between $T^a(t)$ and $T(t)$, additional disturbance terms (e.g., when a fridge is opened), hourly values of C and R, etc. Nevertheless, (3) serves as a good starting point for a simple TCL model.

Acknowledgement

The authors would like to acknowledge the financial support from Innovation Fund Denmark under grant number 0153-00205B for partially funding the work in this paper. The authors would also like to thank Christian Ahn Albertsen (IBM Client Innovation Center) for all our discussions and his feedback which has been particularly valuable regarding practical challenges faced for demand-response. The authors would also like to thank Bennevis Crowley (DTU) for reading the paper and providing feedback on corrections, figures, and phrases. The authors would also like to thank the Centre for Utilities and Supply at Energistyrelsen (Danish Energy Agency) for allowing us to present our work to them while also elaborating their perspective on Market Model 3.0 and their intentions.

References

[1] He Hao et al. "Aggregate flexibility of thermostatically controlled loads". *IEEE Transactions on Power Systems* 30 (1) (2014), pages 189–198.

Author Biographies

Peter A.V. Gade is an Industrial PhD researcher at IBM and affiliated with the Technical University of Denmark, Kongens Lyngby, Denmark, in the Energy Markets and Analytics Section within the Power and Energy Systems division at the Wind and Energy Systems Department. His research focuses on demand-side flexibility and the revenue streams from utilization of demand-side flexibility. He holds a M.S. in Mathematical Modelling and Computing and a B.S. in Biomedical Engineering, both from the Technical University of Denmark.

Trygve Skjøtskfit is an Associate Partner at IBM Denmark, with focus on energy transformation and demand-side flexibility. His solid experience and deep knowledge within intelligent energy systems, buildings, and civil infrastructures makes him a leading figure, strategic advisor, and a first mover in the flexibility market with a strong track record to find and deliver new cutting-edge solutions. He holds an MBA in Strategy from Universitat Pompeu Fabra, and a Master of Export Engineering from Copenhagen University, College of Engineering.

Henrik W. Bindner received the MSc in Electrical Engineering from Technical University of Denmark in 1988. He is currently a senior researcher with the Department of Wind and Energy Systems, Technical University of Denmark. He is heading the *Distributed Energy Systems* Section and his research interests include control and management of smart grids, active distribution networks, and integrated energy systems.

Jalal Kazempour is an Associate Professor with the Department of Wind and Energy Systems, Technical University of Denmark, where he is heading the *Energy Markets and Analytics* Section. He received the Ph.D. degree in Electrical Engineering from the University of Castilla-La Mancha, Ciudad Real, Spain, in 2013. His research interests include intersection of multiple fields, including power and energy systems, electricity markets, optimization, game theory, and machine learning.